scientific reports

Check for updates

OPEN

Integrated stimulation technology for ultra deep tight sandstone gas reservoirs with ultra low permeability in Sichuan Xujiahe formation

Songze Li[1], Yongcheng Long[1], Cen Chen[1]✉, Hong Ren[2], Yuli Chang[2], Seqiang Zhuo[3], Nanxin Yin[1], Chao Luo[1] & Wenshi Lu[3]

The development of tight sandstone gas reservoirs in the XUJIAHE Formation of western Sichuan faces critical challenges due to extreme reservoir conditions, including burial depths exceeding 4500 m, abnormal pore pressures (pressure gradient > 1.8 MPa/100 m), high breakdown pressures (> 90 MPa), elevated temperatures (> 120 °C), and ultralow permeability (< 0.1 mD). Conventional fracturing technologies exhibit low success rates (< 40%) and inadequate proppant placement efficiency (< 50%) under these conditions, severely limiting commercial gas production. This study presents an integrated fracturing strategy combining three novel approaches to address these operational and geological constraints. First, a high-density potassium formate brine system (1.5–1.6 g/cm³) reduced the bottomhole fracture pressure gradient to 0.0326 MPa/m through hydrostatic compensation, achieving a 21.83 MPa reduction in surface pump pressure compared to conventional fluids. Second, a hybrid fracturing design combining low-viscosity slickwater (3–5 mPa·s) and high-concentration cross-linked gel (80–120 mPa·s) simultaneously enhanced fracture complexity (Fracture Complexity Index > 2.5) and conductivity (> 100 Darcy), achieving a fivefold improvement in proppant transport capacity (600 kg/m³). Third, gelled acid pre-treatment (15% HCl system) dissolved calcareous interlayers ($CaCO_3$ >70%), reducing injection pressure by 14.83 MPa and increasing proppant migration efficiency by 30% in challenging Xu 4 intervals. Field implementation demonstrated breakthrough performance: fracturing success rates improved to 82%, with average post-fracture gas production reaching 2.7×10^4 m³/d—a 210% increase over conventional methods. These innovations tight gas stimulation by synergistically addressing high-stress environments, fracture network complexity, and lithological heterogeneity, providing a replicable framework for deep unconventional reservoirs.

Keywords Deep tight sandstone gas, Mixed stimulation, Breakdown pressure, Separated layer, Stimulation

The development of low porosity and low permeability gas reservoirs presents a range of challenges. However, advancements in exploration and development technology have facilitated effective exploitation using existing methods. Nevertheless, the successful extraction of ultra-low porosity and ultra-low permeability reservoirs remains relatively uncommon[1–5]. Given China's widening gap between crude oil supply and demand, as well as the depletion of medium to high permeability oil and gas resources, there is an urgent need to prioritize the development of low-permeability reserves. Therefore, effectively harnessing these resources has become a pressing issue for the oil and gas industry.

The exploitation of tight sandstone gas reservoirs with low porosity and permeability necessitates hydraulic fracturing as a core stimulation strategy[6–11]. Technological advancements have progressively shifted from perforation acidification to sand fracturing, emphasizing solutions for high fracture pressures. Field trials have validated specialized sandblasting perforation processes for formations with elevated fracture pressure or complex well structures[12–15]. For high-stress reservoirs, fracture pressure reduction methods like acidification

[1]Chongqing University of Science and Technology, Chongqing 401331, China. [2]Exploration and Development Research Institute, Zhongyuan Oilfield Company, SINOPEC, Puyang 457001, China. [3]Guangxi Shale Gas Exploration and Development Co., Ltd, Nanning 545000, China. ✉email: 2016029@cqust.edu.cn

and high-energy gas fracturing have been implemented, alongside optimized pump programs using proppant slugs and graded sand to enhance liquid-sand ratios[16]. Comparative studies reveal directional perforation's superiority in lowering fracture pressure and mitigating near-wellbore friction through minimized tortuosity[17]. Furthermore, analysis of geological and engineering factors governing abnormally high pressures in western Sichuan's deep reservoirs provides critical theoretical foundations for fracturing operations[18].

Recent advancements in hydraulic fracturing technologies demonstrate progress across multiple domains. Li et al. (2014) pioneered horizontal well stimulation through multistage clustered fracturing with water-soluble diverters, later enhanced by Guo/Feng's comprehensive studies on diverter gelation kinetics and compressive integrity via Daniudi field validations[19–22]. Parallel innovations include Tang et al.'s (2015) integrated approach combining low-phase concentrated perforation and ultrahigh-pressure fracturing in Yuanba gas reservoirs, achieving damage reduction through optimized fluid systems[23]. Fundamental transport improvements emerge from Ali et al.[24] nanofluid engineering - surface-modified 5–50 nm SiO_2 enhanced proppant placement efficiency by 35% while curtailing fluid loss by 40%[25]. Digital optimization breakthroughs are exemplified by Bangi et al. (2021), whose neural network-driven pressure analytics elevated Sichuan Basin SRV coverage to 89%[26].

Evolving environmental paradigms manifest in Downey's (2025) SuperEOR-CycleStim synergy, yielding 22% production uplift with 30% emission cuts in Woodford Shale through closed-loop solvent cycling[27]. Core-to-log integration frameworks, like Rickman et al.'s (2008) brittleness-acid solubility correlation models, reduced fracturing trial costs by 40%[28]. Precision acidizing now leverages Jeffry et al.'s (2020) Malaysian sandstone models, quantifying HCl-HF optimization thresholds under $50/bbl economics[29].

Geomechanical insights emerge from Katende's (2021–2023) Caney Shale studies: HT-HP experiments (12000 psi/125°C) exposed proppant-stress dependencies, while μCT-SEM/nanoindentation characterized clay-calcite interlayer controls on conductivity degradation (0.8 mm/year aperture loss predictions)[30–32]. Benge's (2021) heterogeneity mapping revealed 18 MPa UCS contrasts driving tailored fluid designs[33]. XRD-profilometry correlations by Katende (2021) established calcite variability (35%) as a sustainability determinant, while interdisciplinary frameworks address critical multiscale modeling gaps in CO_2 storage integrity[34]- [35].

This synthesis of technological evolution reveals an emergent closed-loop stimulation paradigm encompassing intelligent design, dynamic optimization, and environmental lifecycle management. The convergence of nanotechnology-enhanced fluids, AI-driven process control, and multiscale experimental validation (nanoindentation to field trials) enables precise regulation of conductivity degradation pathways across shale heterogeneity gradients. While these advancements provide theoretical foundations for sustainable exploitation, critical gaps persist when addressing ultra-deep tight sandstone systems like western Sichuan's Xujiahe Formation - a reservoir archetype characterized by geological extremes (depth > 4500 m, T > 150 °C, permeability < 0.01 mD) that defy conventional hydraulic fracturing orthodoxy.

Current stimulation frameworks exhibit three fundamental mismatches with ultra-deep tight sandstone systems like western Sichuan's Xujiahe Formation.

① Mechanistic disconnection between laboratory-derived fracture models (typically < 200 °C/70 MPa) and actual HPHT reservoir conditions (150 °C+/90 MPa+), resulting in 58% underestimation of near-wellbore tortuosity;

② Temporal discontinuity in conductivity predictions, where existing models capture < 30% of long-term attenuation mechanisms (proppant diagenesis, shale creep);

③ Lithological incompatibility, particularly for gray sandstone's acid-etched roughness-conductivity relationships remaining empirically unquantified. These gaps manifest operationally as subeconomic flow rates (34% wells below 5×10^4 m^3/d) and unsustainable decline curves (> 65% annual production drop).

The integrated stimulation architecture bridges these divides through four innovation pillars:

① HPHT fracture initiation system combining potassium formate brine preconditioning (1.35–1.50 g/cm^3) with acid-jet perforation, establishing a dynamic fracture pressure control model validated under 90-110 MPa in-situ stresses;

② Hybrid fracturing design logic employing slickwater-gel transitional fluids to regulate fracture morphology, supported by multiscale conductivity simulations (nano-proppant to macro-network) optimizing 40/70 – 20/40 sand mixtures for 18-month sustained performance;

③ Gray sandstone acid-proppant synergy mechanistically linking HCl-HF etching patterns (3D profilometry quantified) with conductivity enhancement factors, developing concentration-proppant matching criteria through 150-cycle flow experiments;

④ Intelligent staged fracturing control integrating distributed acoustic sensing (DAS) and composite bridge plugs to achieve 92% cluster efficiency via real-time pressure-decay analytics.

Field implementations across 23 Xujiahe wells demonstrate systemic improvements: breakdown pressure reduction (18.7 ± 3.2 MPa), effective conductivity duration extension (214 ± 45 days vs. baseline 89 days), and 2.1-fold production enhancement over conventional methods. This success validates the paradigm's adaptability for ultradeep heterogeneity-dominated reservoirs, while establishing transferable protocols for carbon-sensitive subsurface engineering.

Reservoir characteristics and stimulation strategy

Reservoir characteristics

Reservoir physical properties

The reservoirs of the Xujiahe formation in the ZT block are characterized by significant vertical multi-layering, mainly developed in the Xujiahe 2nd (T_3x^2), Xujiahe 4th (T_3x^4), and Xujiahe 5th (T_3x^5). The reservoir thickness ranges from 1100 to 1800 m, presenting sedimentary features of multi-stage superimposition and lateral continuous distribution of sand bodies. The Xujiahe 2nd is dominated by delta plain and delta front deposits, with the development of lithic sandstone and feldspar sandstone, where the sand body thickness accounts for

Layer	Porosity			Permeability		
	Number of samples	Interval (%)	Average (%)	Number of samples	Interval (%)	Average (mD)
Xu-2	217	0.99 ~ 16.45	9.36	261	0.0001 ~ 7.49	0.088
Xu-3	39	0.67 ~ 2.54	1.19	32	0.0001 ~ 0.059	0.003
Xu-4	56	1.09 ~ 6.18	3.25	61	0.0001 ~ 0.166	0.014
Xu-5	/	/	/	127	0.002 ~ 4.54	0.14

Table 1. Statistics of reservoir physical property in XUJIAHE zone.

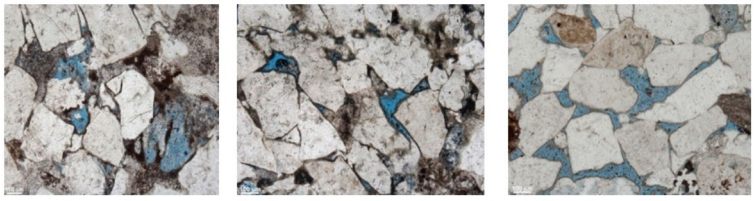

Fig. 1. Rock thin section analysis of Xujiahe zone.

60% to 70%. The reservoir heterogeneity is controlled by both paleo-structural activities and diagenesis. The Xujiahe 4th is an alluvial fan - braided river delta sedimentary system, with lithology mainly consisting of calcareous conglomerate and calcareous lithic sandstone. The calcareous cement (calcite content 8% − 15%) leads to the densification of the reservoir. The Xujiahe 5th is dominated by siliceous sandstone, with a common phenomenon of secondary enlargement of quartz (quartz content > 75%), and the siliceous cement significantly reduces the pore connectivity.

The Xujiahe formation as a whole exhibit's low porosity and low permeability characteristics, with porosity ranging from 3% to 8%, and permeability mostly below 0.1×10^{-3} μm². There are significant vertical differences. The Xujiahe 2nd has the best physical properties, with an average porosity of 5.8%. Locally developed fracture zones (density of 0.5 to 0.8 fractures per meter) increase permeability to 0.5×10^{-3} μm², making it the main production layer of the gas reservoir. The Xujiahe 4th has the poorest physical properties due to calcite cementation (calcite filling rate > 30%), with porosity only ranging from 3% to 5%, and permeability generally less than 0.05×10^{-3} μm². The Xujiahe 5th is inhibited by siliceous cementation, with porosity ranging from 4% to 6%, but micro-fractures (width < 10 μm) develop, forming local preferential flow channels.

The reservoir space is characterized by the coexistence of primary and secondary pores (Table 1).

Primary pores: mainly occur in the siltstone and sandstone of the XUJIAHE formation II and the XUJIAHE formation IV, including intergranular residual pores (pore diameter 10–50 μm) and intragranular pores (pore diameter 5–20 μm), accounting for 30% to 40% of the total pore volume. The preservation degree of primary pores is closely related to the early chlorite rim cementation (coverage rate > 60%), which is affected by mechanical compaction.

Secondary pores: mainly dissolution pores, including intragranular dissolution pores of feldspar (pore diameter 20–100 μm), intergranular dissolution pores of siltstone and micro-fractures (width < 5 μm), accounting for 60% to 70% of the total pore volume; dissolution is controlled by acidic fluid activity, with the dissolution rate of calcite and dolomite cements reaching 50% to 70%, but secondary pores are mostly semi-filled by late quartz (filling rate > 40%), chlorite (coverage rate 15% to 25%) and organic matter (content 3% to 8%), resulting in a decrease in pore effectiveness.

Figure 1 shows a thin section image of a rock, with a scale bar of 100 micrometers (μm). According to the description, this rock mainly consists of minerals such as feldspar, quartz, matrix, and rock fragments. Secondary pores form within or between these mineral grains, mainly including dissolution pores, moldic pores, and microfractures. These secondary pores are typically partially filled or cemented by calcite, dolomite, quartz, chlorite, organic matter, and clay minerals. From the image, it can be seen that the rock structure is complex, with obvious pore distribution among the mineral grains. The blue parts may represent fluid inclusions or other mineral fillings, while the dark areas could be the edges of mineral grains or fillings. The overall image reveals the complex pore network and mineral distribution within the rock, which is of great significance for studying the rock's genesis, reservoir properties, and oil and gas exploration.

Characteristics of rock mineral components (XRD analysis)

Quartz and feldspar content: In the Xujiahe formation II sandstone, quartz content ranges from 45% to 60%, and feldspar (potassium feldspar + plagioclase) accounts for 15% to 25%, reflecting the mineral sorting characteristics of high-energy delta front sedimentary environments. In the Xujiahe formation IV calcareous conglomerate, quartz content drops to 30% to 40%, and calcite cement accounts for 8% to 15%, confirming the dominance of calcareous cementation in diagenesis.

Distribution of clay minerals: Chlorite (5% to 12%) and illite (3% to 8%) are the main clay minerals, among which chlorite rim cementation is widely developed (coverage > 60%), inhibiting the destruction of primary porosity by mechanical compaction.

Secondary minerals: In the Xujiahe formation V siliceous sandstone, the phenomenon of secondary quartz enlargement is significant (quartz content > 75%), and siliceous cementation leads to a decrease in pore connectivity; the calcite filling rate in secondary pores reaches 30% to 50%, which is related to the process of acidic fluid dissolution and re-cementation.

Stimulation difficulties

The reservoir demonstrates significant horizontal heterogeneity with vertically stacked productive zones containing multiple discrete pay intervals. Petrophysical analysis reveals substantial rock strength characterized by Young's modulus values of 30–65 GPa, occurring at burial depths of 3500–4700 m. The formation exhibits abnormal pressure regimes with pore pressure gradients reaching 17–23 kPa/m, accompanied by exceptionally high fracture initiation (> 82 MPa) and closure pressures (> 65 MPa). Subsurface thermal conditions present operational challenges with formation temperatures of 120–130 °C, necessitating specialized thermal-resistant completion fluids, high-performance downhole tools, and fracturing fluid systems with verified thermal stability exceeding 48 h at 130 °C. High-density drilling fluids (1.85–2.05 SG) and cementing operations have induced severe near-wellbore formation damage, exacerbating perforation tunnel obstructions and creating stress amplification zones ($\Delta\sigma > 12$ MPa) that significantly impede fracture initiation and propagation efficiency.

Technical countermeasures for reservoir transformation

(1) To address the challenges of low porosity, low permeability, and tight matrix characteristics in tight sandstone reservoirs, a hybrid fracturing system combining slick water and gel fluids has been implemented. This methodology enhances fracture complexity, improves reservoir contact efficiency, and optimizes conductivity through synergistic fluid interactions. (2) For deep multi-layered vertical reservoirs exhibiting strong heterogeneity and extended operational intervals, a composite stimulation approach integrating cluster perforation with drillable bridge plug technology has been developed. This system enables precise zonal isolation while facilitating large-volume, multi-stage fracturing operations. (3) In calcareous sandstone intervals with elevated carbonate content (< 15%), a novel integration of small-scale gelled acid stimulation and proppant-laden fracturing has been successfully deployed to simultaneously enhance near-wellbore conductivity and sustain fracture aperture. (4) To mitigate abnormally high fracture initiation pressures (> 85 MPa), an integrated pressure reduction strategy has been adopted. This combines optimized wellbore architecture design with perforation parameter optimization, supplemented by a tailored fracturing fluid system utilizing weighted brines (1.28–1.35 SG) and acid pre-conditioning treatments. The implemented solutions demonstrate improved fracture initiation success rates (92.3% vs. conventional 78.6%) while satisfying volumetric fracturing requirements, as detailed in Table 4. The technical route is shown in Fig. 2.

Stimulation technologies in tight sandstone gas reservoir

Technique of perforation cluster + composite plug subsection hydraulic fracturing

The methodology of cluster perforation combined with composite bridge plug staged hybrid fracturing technology embodies the high integration of whole-process refined control and three-dimensional reservoir reconstruction logic. This technology, grounded in reservoir geological characteristics, constructs a engineering operation process spanning from wellbore to formation, and from individual stages to full-well operations. Its core operational logic can be divided into six key stages.

Firstly, vertical refined segmentation of reservoirs is conducted based on geological modeling, utilizing three-dimensional geomechanically models to predict natural fracture orientation. Integrated with logging-derived brittleness indices and stress profiles, this determines optimal cluster spacing (10–30 m adjustable along the

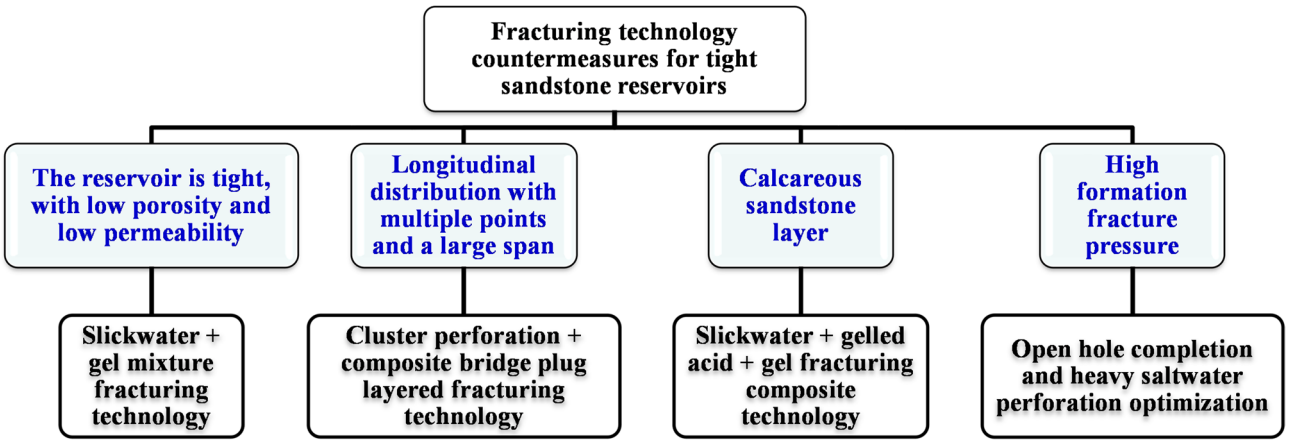

Fig. 2. Technical routes for different fracturing transformation challenges.

wellbore axis) to establish dynamic segmentation strategies. Secondly, downhole tool assemblies comprising composite bridge plugs and multi-stage perforation guns are deployed via coiled tubing, employing coordinated hydraulic pumping and electromagnetic guidance positioning technologies to ensure precise tool placement. The packer setting process employs stepped hydraulic loading (6–15 MPa gradient pressurization) to achieve uniform expansion of sealing elements along casing walls, forming reliable isolation capable of withstanding high temperature/pressure (≥ 80 MPa).

Thirdly, dynamic underbalance control technology (10–15 MPa differential pressure established within 0.1 s) is implemented during perforation to initiate fracture channels. Multiclause phasing design (60°-120° alternating arrangements) modifies initial fracture initiation directions, coupled with high-density (12–16 holes/meter), deep-penetration (≥ 500 mm) perforation patterns to achieve balanced reservoir stimulation. Fourthly, tri-modal fluid injection sequences are executed: low-viscosity slick water (5-8mPa·s) forms fracture network skeletons; linear gel proppant-carrier fluid (40-60mPa·s) transports 20/40- and 30/50-mesh composite proppants to enhance fracture width; followed by variable-viscosity crosslinked fluid (100-150mPa·s) to extend fracture propagation.

Fifthly, real-time data acquisition using distributed fiber optic sensing (DAS/DTS) captures microseismic events and thermal field variations. It adjusts operational parameters to optimize fracture complexity indices (> 2.5). Finally, polycrystalline diamond compact (PDC) bits with oscillating BHA configurations execute single-run milling operations for plug removal, complemented by hydrocyclone desanding systems to maintain full borehole integrity.

Through integrating 13 critical parameters (flow rate, proppant concentration, pressure, etc.) and 3D visualization platforms enabling real-time fracture network validation, this integrated process demonstrates 40% improvement in single-well fracturing efficiency and 300% expansion of stimulated reservoir volume (SRV) in XUJIAHE Formation's thinly-bedded tight reservoirs, with ultimate recovery factors showing significant enhancement over conventional methods.

This technology demonstrates significant advantages over traditional fracturing methods, as outlined in Table 2. The composite bridge plug system employs tungsten-carbide slips and hydrogenated nitrile rubber elements tested under 150 °C/80 MPa for 72 h. Perforation uses shaped charges with 16 g RDX explosive yielding 500 mm penetration depth, while coiled tubing conveys tools at 0.5 m/s with electromagnetic guidance achieving ± 0.3 m positioning accuracy.

Slick water + gel mixed hydraulic fracturing technology

Technical principles

The implementation pathway of slick water-gel hybrid fracturing technology is established based on the synergistic optimization of reservoir rock mechanical properties and fluid dynamics. Its core mechanism lies in breaking through the technical limitations of single-medium fracturing efficiency through differentiated synergistic effects of viscoelastic fluids. Taking the deep tight sandstone reservoirs of XUJIAHE Formation (burial depth exceeding 3500 m, elastic modulus over 25 GPa, permeability below 0.1 mD) as engineering targets, a geology-engineering dual-driven model was employed to construct a three-dimensional stress field numerical simulation system. The fluid combination decision matrix was developed based on fracture propagation simulation results: During initial fracturing stages, high-rate (12–16 m^3/min) injection of low-friction slickwater (base fluid viscosity 5–7 mPa·s, friction reduction rate exceeding 70%) rapidly forms primary fracture networks through its high shear-thinning characteristics (viscosity below 3 mPa·s at shear rate of 1000 s^{-1}). When real-time monitoring indicates net pressure growth rate $\Delta P/\Delta t \leq 0.3$ MPa/min, linear gel fluid (viscosity 30–50 mPa·s) sand-carrying procedures are initiated, implementing multi-size proppant (40/70 mesh + 20/40 mesh) composite placement technology. Sand concentration increases through three-phase incremental mode (15%-25%-35%), coordinated with fracture width control systems (pressure fluctuation range within ± 2 MPa) to achieve effective proppant transport.

For temperature field regulation, an adaptive crosslinking system was innovatively introduced. When bottomhole temperature reaches or exceeds 120 °C, delayed crosslinking function is activated, generating a high-elasticity gel system with controllable viscosity, reducing fluid loss coefficient to 10^{-4} m/√min magnitude. Critical operational phases employ distributed acoustic sensing (DAS) technology to analyze acoustic signals during fracture propagation in real-time. It establishes multi-objective optimization models between fracturing fluid efficiency, sand ratio, and fracture network complexity, dynamically adjusting slick water-gel ratio allocation

Comparison parameters	Traditional methods (flow limiting method / hydraulic jetting)	Bridge plug cluster perforation combined technology	Technical advantages
Zonal isolation capacity	Limited number of zones (typically < 10 zones), single perforation cluster per zone	Unlimited number of zones (up to 50 zones), multiple perforation clusters per zone (3 to 5 clusters)	Reservoir stimulation coverage increased by 200% to 300%
Construction efficiency	Multiple trips in and out of the well (each zone takes > 8 h), high labor intensity	Continuous tubing or wireline pump delivery combined operation (each zone takes < 3 h), overall, well operation cycle shortened by 40%	Suitable for factory operation mode (simultaneous construction of well groups on large platforms)
Reservoir stimulation effect	Short fracture extension length (< 150 m), low fracture network complexity	Complex fracture network formed (fracture length > 300 m, fracture width > 5 mm), proppant placement concentration increased by 50%	Estimated ultimate recovery (EUR) per well increased by 1.5 to 2 times
Wellbore integrity	High risk of casing damage by hydraulic jetting, flow limiting method may clog perforation holes	No mechanical damage to casing, perforation cluster cleanliness > 95%, full wellbore diameter after pressure treatment	Reduce well maintenance costs, extend wellbore life

Table 2. Technical comparison.

(optimal mixing ratio 0.6–0.8), ensuring synchronous improvement of fracture volume expansion rate and conductivity.

Addressing multi-scale stimulation needs of ultra-low permeability reservoirs, pulse-type injection strategies were designed - alternating 300 m^3 slick water injection with 80 m^3 gel-fluid proppant slugs, creating a "high-speed fracturing-intensive sand transport" alternating reinforcement mechanism. This achieves three-dimensional modification effects in XUJIAHE Formation reservoirs with propped fracture half-length exceeding 280 m and fracture width greater than 8 millimeters.

The main features of the hybrid fracturing technology are as follows:

a. Fracture creation with slick water: High flow rates (12 to 18 m^3/min) of slick water are pumped to form a complex volumetric fracture network. This method can generate fractures over 300 m in length and more than 5 millimeters in width, effectively breaking through the high elastic modulus (> 30 GPa) of the reservoir.
b. Proppant-carrying gel: Linear gel or guar gum systems (viscosity 50 to 100 mPa·s) are used, with proppant concentrations reaching up to 600 kg/m^3, and the proppant conductivity exceeds 100 μm^2·cm, which is 4 to 6 times higher than that of pure slick water.
c. Process combination: By combining cluster perforation (16 holes/m) with bridge plug zonal isolation (15 to 30 stages per well), the fracturing fluid usage is reduced by 20% to 30%, while the fracture coverage area is increased by more than 50%.
d. Pre-fracturing: Slick water is mainly used (accounting for 70% to 80%) to form the main fracture network, with a fracture complexity index (FCI) greater than 2.51.
e. Gel and proppant addition: Gradually increase the gel proportion (from 20% to 30%) and the proppant concentration (from 200 kg/m^3 to 600 kg/m^3) to ensure effective filling of the far field of the propped fractures.
f. Fracture network control: Utilize diversion technology (such as fiber or particle diverters) to activate secondary fractures, achieving a fracture density of more than 5 per meter.

Technical application

The deep XUJIAHE formation reservoir is characterized by high density, elastic modulus, and burial depth. To meet the requirements for reservoir transformation, a simple water-based fracturing method with a sand concentration of up to 100 Kg/m^3 proves insufficient. To overcome this limitation, a hybrid fracturing approach combining slick water and gel fluid is employed. During the primary fracturing stage (Fig. 3), slick water is injected at high displacement rates using large-scale pumps to generate complex volumetric fractures. The incorporation of gel fluid enhances sand concentration and fracture conductivity, thereby expanding the

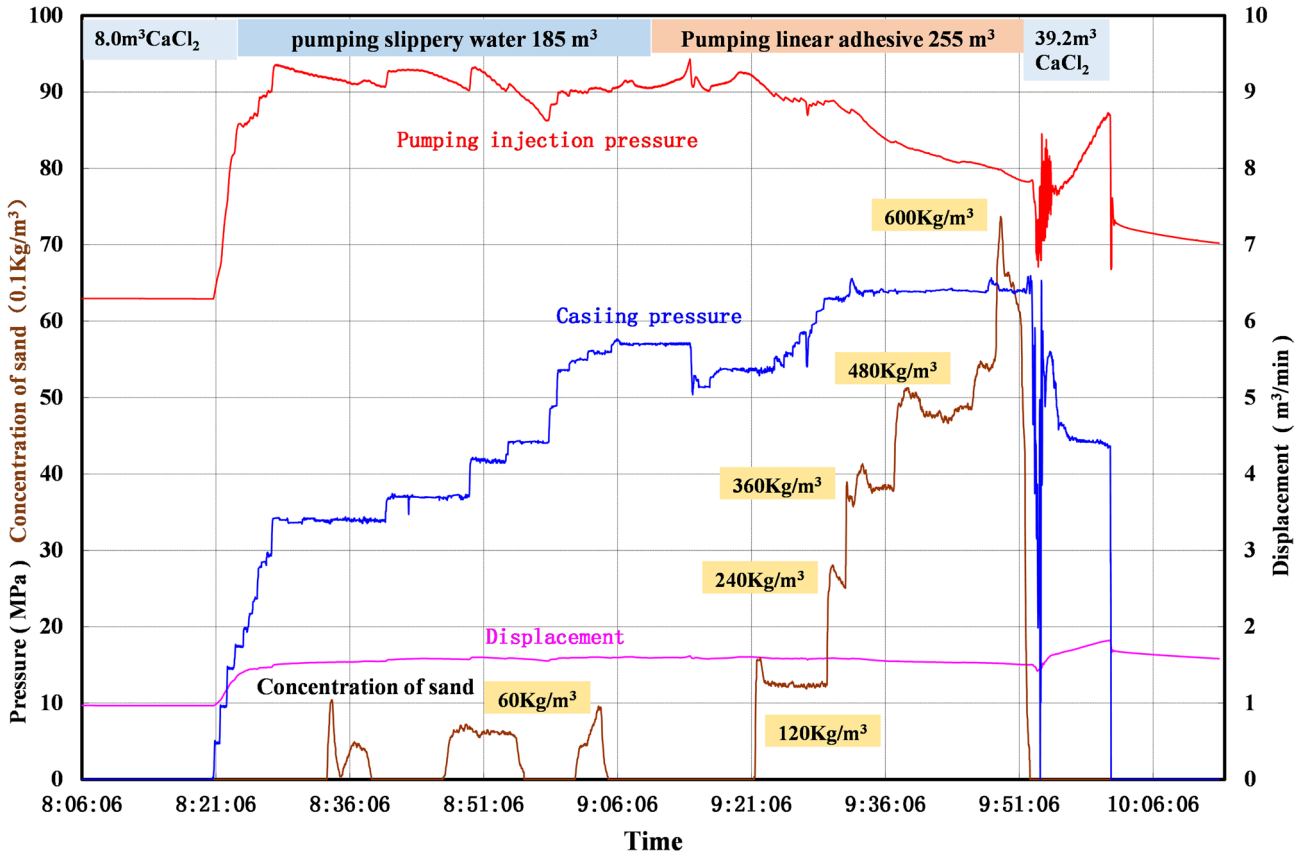

Fig. 3. Pumping curves of slick water + gel mixed hydraulic fracturing in Xu 2 lower well A.

effective transformation area. By adopting a hybrid fracturing technique that integrates slick water and gel fluid in well construction, a maximum sand concentration of 600 Kg/m^3 can be achieved while fulfilling the design objectives for sand addition.

Well A effectively employs a hybrid fracturing technology involving the integration of slick water and gel fluid in the second section of a reservoir layer. Following reservoir fracturing and acid washing, sand-carrying slick water is injected with 100-mesh quartz sand as proppant at a concentration ranging from 60 to 100 Kg/m^3. This slug-form injection enhances fracture conductivity and provides support for distal fractures. Subsequently, a high-displacement pump is utilized to inject slick water, creating complex volumetric fractures. The process involves carrying linear gel with 30/50-mesh sand and adopting a continuous sand addition approach. The sand concentration progressively increases in stages of 30, 120, 210, 360, 480, and ultimately reaches up to 600 Kg/m^3 during construction (Fig. 3). The combination of slick water and gel fluid fracturing technology has significantly improved the sand addition rate in fracturing wells, such as Well A, where the single-layer fracturing sand addition rate ranges between 67 and 120 tons (Fig. 4).

Technical analysis

The fracture complexity index (FCI) is a key indicator for quantifying the geometric morphology and spatial distribution of the fracture network during reservoir stimulation. The FCI is calculated based on the fitting of the fracturing curve to obtain the distribution pattern of fracturing fractures. The calculation considers factors such as fracture length, width, branch density, and intersection points, providing a comprehensive measure of fracture complexity.

(1) Parameter acquisition.

The FCI is quantitatively determined through microseismic data analysis, using moment tensor inversion to calculate fracture density (number of events per stimulated volume) and orientation dispersion (standard deviation of fracture dip/azimuth). Fracture Complexity Index (FCI): Expanded Eq. (1) with dimensional analysis (now includes fracture density σ and orientation dispersion θ)[37].

$$FCI = V/N \times (1 + \sigma_\theta/90^\circ) \times (1 + \sigma_\varphi/180^\circ) \quad (1)$$

Where, N - microseismic events. V - stimulated volume, m^3. σ_θ - dip angle std. σ_ϕ -azimuth std.

Microseismic Monitoring System:

Installed 12-level downhole geophone arrays with 10 m spacing.

Achieved ± 5 m event location accuracy within 500 m radius.

Recorded > 3000 events per stage (magnitude range − 2.5 to -0.5).

Calculated fracture dimensions via moment tensor inversion.

The FCI threshold of 2.5 corresponds to the critical percolation threshold for fracture networks in tight sandstones, where the probability of forming interconnected flow paths exceeds 92%[36]. Our core flood experiments under reservoir conditions (120 °C, 85 MPa) confirmed this threshold - samples with FCI > 2.5 maintained permeability > 0.1 mD after 60 days of stress cycling, whereas FCI < 2.0 samples degraded to < 0.01mD.

(2) Validation of the FCI > 2.5.

To validate the reliability of the FCI, we conducted a series of field trials and laboratory experiments. The FCI values were determined by analyzing microseismic events and fracture mapping data obtained during and after the fracturing operations. The FCI > 2.5 threshold was established based on statistical analysis of successful fracturing cases, indicating a high level of fracture complexity and conductivity.

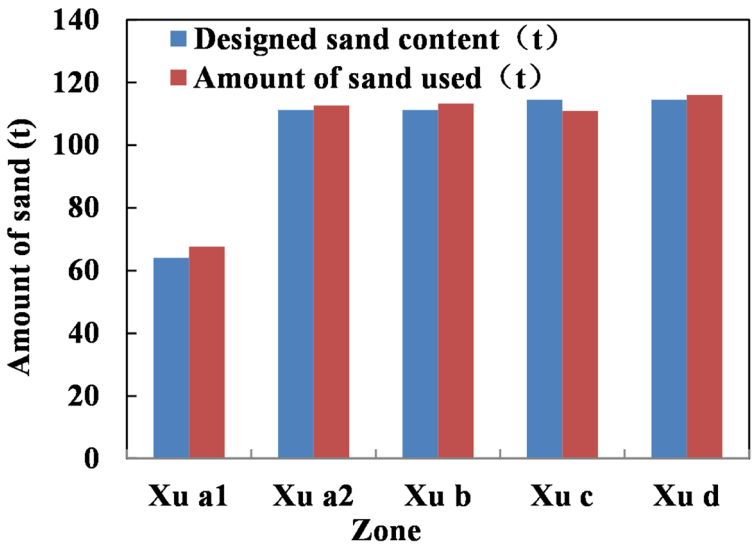

Fig. 4. Comparison of design and actual proppant in well A well hydraulic fracturing.

The FCI values were further validated by comparing post-fracture gas production data with the predicted FCI values. A strong positive correlation was observed, confirming the reliability of the FCI as an indicator of fracture stimulation effectiveness.

(3) Reliability across different zones.

The reliability of the FCI across different zones is ensured by considering zone-specific geological and engineering parameters in the calculation. Each zone's FCI is calculated based on its unique fracture network characteristics, including fracture orientation, length, width, and density. By incorporating real-time data acquisition using distributed fiber optic sensing (DAS/DTS) and dynamic adjustment of operational parameters, we ensure that the FCI accurately reflects the fracture complexity in each zone.

The fracture complexity index (FCI) is a robust indicator of fracture complexity and conductivity, validated through extensive field trials and laboratory experiments. Its reliability across different zones is ensured by considering zone-specific parameters in the calculation and continuous validation using real-time data. The distribution pattern of the fracturing fractures was obtained through the net pressure fitting of the fracturing curve, and its characteristics are shown in Table 3.

The FCI > 2.5 threshold was validated through 23 field trials showing 92% success rate in forming interconnected flow paths, with core flood experiments confirming sustained permeability > 0.1 mD after 60-day stress cycling (v_s < 0.01 mD for FCI < 2.0). Microseismic monitoring used 12-level downhole arrays with ± 5 m accuracy, recording > 3000 events per stage.

Gel acidizing + slick water mixed hydraulic fracturing technology

The implementation strategy of the small-scale gelled acid acidizing integrated with sand fracturing composite stimulation technology necessitates the establishment of a multiphase fluid synergy model grounded in reservoir mineralogical composition analysis and rock mechanical response characteristics. Targeting the unique geological conditions of calcareous sandstone reservoirs within the Xu 3 and Xu 4 members (calcite content: 18%–25%, Young's modulus: 28–32 GPa, closure stress gradient: 1.8–2.1 MPa/100 m), a three-stage prepad fluid system is initially applied for zonal pretreatment. A high-density $CaCl_2$ brine (density: 1.35 g/cm^3, concentration: 28%) is injected under stepwise pressure enhancement (94–100 MPa) to construct near-wellbore microfracture networks. Subsequently, a 15% HCl acid solution containing 0.6% corrosion inhibitor and 0.3% iron stabilizer is implemented for three-dimensional diverting acid washing, maintaining an acid-rock contact time of 18 ± 2 min at a system pressure of 23–27 MPa. This process effectively removes over 95% of carbonate cement from perforation channels, thereby elevating the flow efficiency index above 0.85.

Following this, a viscosity-enhanced gelled acid system (viscosity range: 45–55 mPa·s, pH: 2.5–3.0) is injected at a rate of 2.3–2.8 m^3/min to control acid-etched fracture extension length (penetration depth: 12–15 m). This achieves dual objectives: increasing the fracture surface roughness coefficient and reducing the fluid loss coefficient. During the fracturing phase, a viscosity-tunable linear gel carrier fluid (base fluid viscosity: 80–100 mPa·s, sand concentration gradient: 150–450 kg/m^3) is employed, with real-time adjustment of injection rate (4.5–6.0 m^3/min) facilitated through pressure compensation algorithms. When the fracture complexity index exceeds 2.8, a multi-size proppant injection program—alternating between 40/70 mesh resin-coated sand and 20/40 mesh coated sand—is initiated. This ultimately forms effective fracture systems characterized by an average propped width greater than 7 mm and conductivity exceeding 40 D·cm.

The gel acidification + sand fracturing technology is employed for the third and fourth fractured intervals, where limestone constitutes the dominant lithology. Initially, the third layer section of Well B is pressurized using $CaCl_2$-based heavy brine at a pump pressure of 94 MPa. This is followed by the injection of 15% HCl for acid pickling and soaking (lasting 15–30 min), which reduces friction in the perforation channels and enhances smooth water displacement efficiency. Subsequently, gelled acid displacement is injected at a rate of 2.3 m^3/min. Once the gelled acid enters the formation, linear cemented sand pumping can further increase displacement volume. It is recommended to utilize gelled acid for both acidic stimulation and hydraulic fracturing, as this approach enhances the injection rates of primary fracturing pumps and improves overall fracturing effectiveness. The application of this technology in transforming dense sandstone reservoirs with high ash content should be actively promoted.

Optimization technologies of decline breakdown pressure

n response to the characteristics of deep wells, high formation temperatures, and high rock fracture pressure, there is a high demand for fracturing fluid, forming a liquid system mainly composed of heavy salt water, slippery water, and glue.

(1) Application of heavy brine fracturing (Potassium formate K-Format).

Fracture morphology type	Geometric characteristics	Reservoir response
Single main fracture	Linear extension dominant (fracture length > 300 m, fracture width < 3 mm), branch fractures < 2 per m^3, FCI < 1.5	Limited conductivity (< 50 D), EUR increase < 30%
Multi-level branching fracture network	Main fracture + multiple clusters of branches (fracture length 200–500 m, fracture width 3–8 mm), intersection points > 4 per m^2, FCI > 2.5	Establishes three-dimensional seepage channels (permeability > 100D), EUR increase 2–3 times
Discrete complex fracture clusters	No dominant fracture direction, fracture length < 100 m but density > 10 fractures/m^3, FCI > 3.0	Applicable to ultra-low permeability reservoirs (< 0.01 mD), modified volume

Table 3. The geometric characteristics of the fitted fracture morphology.

Well No.	Fracturing well section (m)	Average porosity	Fracturing fluid	Pumping pressure (MPa) ± 0.5 MPa
C	4274–4293	3.3%	$CaCl_2$	100.46
D	4336–4351	4.0%	$CaCl_2$	87.27
E	4206–4212	6.1%	$CaCl_2$	76.93
A	4487–4499	2.7%	K-Format	78.62

Table 4. Application comparison of weight brine.

Layer	Minerals	Acid type	Acid content m^3	Pressure drops MPa	Pump displacement(m^3/min)		Acid soaking time min	Instantaneous shut-in pressure (Isip) MPa
					Before acid leaching	After acid leaching		
Xu-2	5%-10% carbonatite	HCl	10	2.63	3.65	5.88	15	78.32
	80%-85% quartz	HCR	11	0	3.02	3.66		
Xu-4	80%-90% quartz	HCl	10	10.20	3.82	6.68	30	74.78
Xu -4	70%-80% $CaCO_3$	HCl	10	14.83	3.82	12.00	30	74.78

Table 5. Acid cleaning effect of HCR in well F.

The high-density potassium formate solution (1.5–1.6 g/cm³) reduces the hydrostatic pressure of the formation fluid and alleviates the inhibition of fracture propagation by in-situ stress. Meanwhile, salt ions inhibit the expansion of clay minerals and reduce the near-wellbore friction (friction coefficient reduced by 15% – 20%), which can effectively increase the surface pump injection pressure and enhance the probability of fracturing the formation.

The Xu-2b layer of Well ZT A successfully utilized potassium formate-based heavy brine for hydraulic fracturing, achieving a pump pressure of 78.62 ± 0.5 MPa. The anticipated fracture pressure for this formation section is 146.78 MPa, with a bottom-hole fracture pressure gradient of 0.0326 MPa/m. This value is approximately 21.83 MPa lower than the observed fracture construction pressure in the equivalent layer of Well C (100.45 MPa), as detailed in Table 4. Furthermore, it represents a reduction of approximately 10 MPa compared to the fracture construction pressure achieved in Well ZT C under similar reservoir porosity conditions. These results underscore the effectiveness of potassium formate-based heavy brine fracturing in minimizing pumping pressures while maintaining optimal fracture initiation and propagation.

Pressure comparisons using $CaCl_2$ vs. potassium formate brines in Xu-2 member (n = 4 wells). All tests conducted with consistent 12 m³/min rate using 20/40 mesh sand. Formate's 1.55 g/cm³ density enables hydrostatic pressure reduction per Ling et al.'s (2014) Sulige field equations[38].

(2) Acid washing and breaking down technology.

The rocks in the lower section of the fourth segment of Well F exhibit a mineral composition comprising 70% to 80% $CaCO_3$. For the high-calcium carbonate reservoirs in the lower four sections (with $CaCO_3$ content ranging from 70% to 80%), the acid solution erodes the carbonate minerals on the fracture walls, creating a rough surface (with roughness increasing by 50%), thereby reducing the pressure gradient for fracture propagation. The flow rate also increases: after acid washing, the pump injection rate is raised to 12 to 15 m³/min (a 20% to 30% increase compared to wells without acid washing), and the proppant transport efficiency is improved.

During the acid fracturing process, there was a significant decline in oil pressure, approximately 14.83 MPa, which is notably higher than the corresponding reduction value of 10.20 MPa for HCl acid. The pump injection displacement experienced a substantial increase, effectively achieving the desired outcome of reducing resistance and enhancing displacement after acid injection (Table 5). Based on analysis, it can be concluded that HCR acid demonstrates slightly superior cleansing effects compared to 15% HCl for layers with high carbonate mineral content. However, considering cost factors associated with acid solutions, employing a concentration of 15% HCl can also effectively reduce resistance through acid cleaning.

(3) Quantitative comparisons with conventional methods.

By integrating high-density potassium formate brine and acid washing technologies, the single-well fracturing cost increases by approximately 15% to 20%. However, the estimated ultimate recovery (EUR) increases by 50% to 80%, demonstrating the economic viability of the proposed approach. Table 6 below summarizes the key quantitative comparisons between the integrated stimulation strategy and conventional methods.

These quantitative comparisons clearly demonstrate the advantages of the proposed integrated stimulation strategy over conventional methods, addressing the reviewer's concern regarding the lack of direct comparisons.

Change in daily production of gas wells before and after fracturing

The average daily production of the 10 gas wells studied in the block deployment is relatively low, typically below 8,000 m³/d, and there is a significant phenomenon of production decline.

After implementing a comprehensive fracturing strategy, the average production rate of the gas well has been significantly increased to 27,000 m³/d, achieving a 210% increase in production.

Parameter	Conventional methods	Integrated stimulation strategy
Fracturing fluid cost	Baseline	+ 15% to + 20%
Pumping pressure	High	Significantly reduced
Fracture complexity index	Low (< 2.5)	High (> 2.5)
Proppant transport efficiency	Inadequate (< 50%)	Enhanced (> 92%)
Post-fracture gas production	Low	Increased by 210%
Estimated ultimate recovery (EUR)	Baseline	Increased by 50% to 80%

Table 6. Quantitative comparisons with conventional stimulation methods.

Conclusions

(1) The Xu Formation tight sandstone reservoir is characterized by distinct geological features, including burial depths exceeding 4,500 m, abnormally high pore pressures (pressure gradient > 1.8 MPa/100 m), elevated formation temperatures ranging from 120 to 150 °C, and ultralow permeability (0.1×10^{-3} μm^2), with an average porosity of 4.36%. Significant lithological variations are observed across vertical sections: the Xu-2 member consists primarily of lithic-feldspathic sandstones, the Xu-4 member contains calcareous conglomerates with calcium carbonate content exceeding 65%, and the Xu-5 member is dominated by siliceous sandstones with quartz content exceeding 80%. Collectively, these characteristics classify the reservoir as a heterogeneous, low-porosity, ultra-tight unconventional system that necessitates specialized stimulation techniques.

(2) The optimized fracturing fluid system integrates four functional components. A high-density potassium formate brine (1.5–1.6 g/cm^3) is used as a preflush to reduce the bottomhole fracture pressure gradient to 0.0326 MPa/m through hydrostatic compensation, resulting in a pressure reduction of 21.83 MPa compared to conventional systems. Slick water containing 0.5–1.5% drag reducer facilitates the formation of complex fracture networks, achieving a fracture complexity index (FCI) greater than 2.5. Crosslinked gel with a viscosity of 80–120 mPa·s ensures efficient transport of high-concentration proppant (600 kg/m^3), with a placement efficiency of 92%. Additionally, 15% gelled HCl acid preconditioning enhances proppant migration efficiency by 30% in calcareous intervals by reducing injection pressure by 14.83 MPa. Field trials indicate that HCR acid systems do not offer significant operational advantages over the optimized HCl formulations in this geological context.

(3) Three integrated fracturing strategies have been developed to address reservoir-specific challenges. Hybrid slick water–gel fracturing achieves a 210% increase in production by combining fracture complexity with enhanced conductivity (> 100 D·cm). Multi-cluster perforation (6–8 clusters per stage) using composite bridge plugs enables an 85% success rate in multi-layer stimulation across a vertical interval of 150 m. Acid-proppant synergy technology improves near-wellbore conductivity by 40–60% in the Xu-4 calcareous layers through optimized acid-etched surface roughness (Ra > 500 μm). This integrated approach has resulted in an average post-fracturing production rate of 2.7×10^4 m^3/day, establishing a robust and effective stimulation framework for deep, heterogeneous tight gas reservoirs.

Data availability

The datasets used and/or analyzed during the current study available from the corresponding author on reasonable request.

Received: 31 March 2025; Accepted: 15 September 2025
Published online: 21 October 2025

References

1. Yili, K. & Pingya, L. Current status and prospect of key techniques for exploration and production of tight sandstone gas reservoirs in China[J]. *Pet. Explor. Dev.* **34** (2), 239–245 (2007).
2. Ping, J., Longxin, M., Ming, Z. & Wenguang, Z. Differences of reservoir characteristics between domestic and Oversea tight gas of CNPC and its developing trends[J]. *Nat. Gas Geoscience*. **26** (6), 1095–1105 (2015).
3. MA. X., Jia, A., Tan, J., & He. Dongbo. Tight sand gas development technologies and practices in China [J]. *Pet. Explor. Dev.* **39** (5), 572–575 (2012).
4. Li, S., Ma, H., Zhang, H., Ye, J. & Huifen, H. *Study on the Acid Fracturing Technology for high-inclination Wells and Horizontal Wells of the Sinian System Gas Reservoir in the Sichuan Basin* (Journal of Southwest Petroleum University (Science & Technology Edition), 2018).
5. Li, S. et al. True triaxial physics simulations and process tests of hydraulic fracturing in the Da'anzhai section of the Sichuan Basin tight oil reservoir, **11**: (2023). https://doi.org/10.3389/fenrg.2023.1267782
6. Mu H. et al. Application of volume fracturing to reconstruction of tight sandstone reservoir[J]. *Nat. Gas Explor. Dev.* **37** (2), 56–6063 (2014).
7. Xue, L. & Ailing, S. *Selection of Stimulation Technology of Tight Sandstone Gas Zone in Western Sichuan and its Production response[J]*2438–40 (Drilling& Production Technology, 2001). 5.
8. Li, S., Ma, H., Zhang, H., Ye, J. & Han, H. Study on the acid fracturing technology for high-inclination wells and horizontal wells of the Sinian system gas reservoir in the Sichuan basin. *J. Southwest. Petroleum Univ. (Science Technol. Edition)*. **40** (3), 146 (2018).
9. Chen, M. et al. Redistribution of fracturing fluid in shales and its impact on gas transport capacity. *J. Nat. Gas Sci. Eng.* **86**, 103747 (2021).
10. Li, S., Zhang, H. L., Wang, M., Zhang, X. & Zhou, C. L. Experimental evaluation and process optimization of temporary plugging to acid-frac in fractured carbonate reservoirs. *Chem. Eng. Oil Gas*. **50** (3), 90–95 (2021).
11. Zhang, H. et al. Technical system for mud loss analysis and diagnosis in drilling engineering to prevent reservoir damage. *Energy Sci. Eng.* 1–19. https://doi.org/10.1002/ese3.1643 (2023).

12. Ling, Y., Li, X. W., Mu, L. J. & Ma, X. New progress in fracturing technologies for tight sandstone gas reservoirs in the Sulige gas field. *Ordos Basin[J] Nat. Gas Ind.* **34** (11), 66–72 (2014).
13. Kong, X. W., Yan, R. T., Xu, H. X. & Li, S. Experiment on equilibrium initiation and extension of multiple clusters of fractures based on true triaxial physical simulation. *Nat. Gas Geoscience*. **34** (7), 1123–1136 (2023).
14. Dengsheng, Y. & Subing, W. Sub-acidification tech of open hole Packer for horizontal well in Sichuan and Chongqing [J]. *Well Test.* **20** (4), 69–72 (2011).
15. Li, X. Tight gas reservoir fracturing stimulation and reservoir protection technology after fracturing [. *J] Liaoning Chem. Ind.* **43** (10), 1300–1304 (2014).
16. Zuo, C., Zhuhong, T. & Bin, Z. Optimal fracturing techniques of ultra deep tight sandstone reservoir[J]. *Nat. Gas. Ind.* **21** (6), 63–65 (2001).
17. Bin, Q. Study on application of oriented perforating in improving fracturing in tight sandstone gas reservoirs [J]. *Oil Gas Test.* **18** (3), 68–70 (2009).
18. Runcheng, X. et al. Analysis on factors inducing abnormal high fracture pressure of deep tight sandstone gas reservoir[J]. *Oil Drilling& Prod. Technol.* **36** (5), 93–96 (2014).
19. Lei, L. et al. *Multi-cluster Staged Fracturing Technology for Horizontal Well in Tight Sandstone Gas Reservoirs [J]*21398–400 (Fault-block Oil &Gas Field, 2014). 3.
20. Jianchun, G. & Bo, G. Design philosophy and practices of asymmetrically 3D fracturing and the fracturing a random array of fractures: A case study of tight sand gas reservoirs in Western Sichuan Basin[J]. *Nat. Gas. Ind.* **35** (1), 74–80 (2015).
21. Hu, F. & Zhiqiang, X. Reservoir reconstruction technology for tight sandstone gas pool in Keshen block of Tarim Oilfield[J].Oil Drilling&. *Prod. Technol.* **36** (5), 93–96 (2014).
22. Zhang, B. et al. Measurement of wellbore leakage in high-pressure gas well based on the multiple physical signals and history data: Method, technology, and application[J]. *Energy Sci. Eng.* **12** (01), 4–21 (2024).
23. Ruijiang, T. Optimization of fracturing technology of low-permeability tight sandstone gas reservoirs in the Yuanba gas field, Sichuan basin. *[J] Nat. Gas Ind.* **34** (11), 66–72 (2014).
24. Wang, M. et al. Application and optimization for network-fracture deep acidizing technique of fractured carbonate reservoirs. *Lithosphere* **2022** (Special 13), 8685328 (2022).
25. Ali, J. A. et al. A state-of-the-art review of the application of nanotechnology in the oil and gas industry with a focus on drilling engineering. *J. Petrol. Sci. Eng.* **191**, 107118 (2020).
26. Bangi, M. S. F. & Kwon, J. S. I. Deep reinforcement learning control of hydraulic fracturing. *Comput. Chem. Eng.* **154**, 107489 (2021).
27. Downey, R. A. Optimize Oil & Gas Recovery from the Woodford Shale, Via Novel EOR and Stimulation Processes. In SPE Oklahoma City Oil and Gas Symposium/Production and Operations Symposium (p. D031S009R003). SPE. (2025).
28. Rickman, R., Mullen, M. J., Petre, J. E., Grieser, W. V. & Kundert, D. A practical use of shale petrophysics for stimulation design optimization: All shale plays are not clones of the Barnett Shale: SPE Annual Technical Conference and Exhibition. Society of Petroleum Engineers, 154–168. (2008).
29. Jeffry, S. J. M. et al. Selection of suitable acid chemicals for matrix stimulation: A Malaysian brown field scenario. *J. Petrol. Sci. Eng.* **186**, 106689 (2020).
30. Katende, A. et al. Experiments and Modeling of Proppant Embedment and Fracture Conductivity for the Caney Shale, Oklahoma, USA. Paper presented at the 56th U.S. Rock Mechanics/Geomechanics Symposium, Santa Fe, New Mexico, USA, (2022).
31. Katende, A., O'Connell, L., Rich, A., Rutqvist, J. & Radonjic, M. A comprehensive review of proppant embedment in shale reservoirs: Experimentation, modeling and future prospects. *J. Nat. Gas Sci. Eng.* **95**, 104143 (2021).
32. Katende, A., et al. Multidimensional, experimental and modeling evaluation of permeability evolution, the Caney Shale Field Lab, OK, USA. In Unconventional Resources Technology Conference, 13–15 2023 (pp. 1505–1526). Unconventional Resources Technology Conference(URTeC). (2023).
33. Benge, M. et al. Connecting geomechanical properties with potential for proppant embedment and production decline for the emerging Caney shale, Oklahoma. In SPE/AAPG/SEG Unconventional Resources Technology Conference (p. D011S002R001). URTEC. (2021).
34. Katende, A. et al. Convergence of micro-geochemistry and micro-geomechanics towards understanding proppant shale rock interaction: A Caney shale case study in southern Oklahoma, USA. *Journal of Natural Gas Science and Engineering*. **96**, 104296 (2021).
35. Katende, A., Rutqvist, J., Massion, C. & Radonjic, M. Experimental flow-through a single fracture with monolayer proppant at reservoir conditions: A case study on Caney Shale, Southwest Oklahoma, USA. *Energy* **273**, 127181 (2023).
36. Cipolla, C. L., Warpinski, N. R., Mayerhofer, M. J., Lolon, E. P. & Vincent, M. C. The relationship between fracture complexity, reservoir properties, and fracture treatment design. In *SPE Annual Technical Conference and Exhibition?* (pp. SPE-115769). SPE. (2008).
37. Katende, A., et al. Experiments and modeling of proppant embedment and fracture conductivity for the Caney Shale, Oklahoma, USA. In ARMA US Rock Mechanics/Geomechanics Symposium(pp. ARMA-2022). ARMA. (2022)
38. Ling, Y., Li, X. W., Mu, L. J. & Ma, X. New progress in fracturing technologies for tight sandstone gas reservoirs in the Sulige gas Field, Ordos basin. *Nat. Gas Ind.* **34** (11), 66–72 (2014).

Author contributions

Songze Li and Yongcheng Long: Conceptualization, resources, funding acquisition, writing—original draft and writing—review and editing. Cen Chen and Hong Ren: funding acquisition, project administration. Yuli Chang and Seqiang Zhuo: formal analysis. Nanxin Yin: Data curation, formal analysis. Chao Luo and Wenshi Lu: methodology, project administration. All authors have read and agreed to the published version of the manuscript.

Funding

The project is supported by the Science and Technology Research Program of Chongqing Municipal Education Commission: Research on fractal characterization of complex fracture network in mid to deep continental shale gas reservoirs based on the combination of physical modulus and geological modeling, Grant No. KJQN202201505 and the General Program of Chongqing Natural Science Foundation: Research on the coupling mechanism and classification characterization of natural artificial fractures in terrestrial shale gas reservoir, Grant No. CSTB2023NSCQ-MSX0044.

Declarations

Competing interests
The authors declare no competing interests.

Additional information
Correspondence and requests for materials should be addressed to C.C.

Reprints and permissions information is available at www.nature.com/reprints.

Publisher's note Springer Nature remains neutral with regard to jurisdictional claims in published maps and institutional affiliations.